# Determination of Detection Parameters on TDCC Performance

Binhee Kim, *Student Member, IEEE*, and Seung-Hyun Kong, *Member, IEEE*

***Abstract*—Due to the longer PRN code employed in next-generation GNSS (Global Navigation Satellite System), receivers in the signal acquisition process should test a larger number of code phase hypotheses. Recently, to reduce acquisition time and computational complexity, TDCC (Two-dimensional Compressed Correlator) is introduced, and this technique is different from the conventional double dwell search technique in terms of parameters used to reduce acquisition time and computational complexity. Studies for optimizing the performance of TDCC have not been introduced yet, therefore, in this paper, detection thresholds of TDCC are investigated to optimize its acquisition performance. The optimal detection thresholds minimizing the MAT (Mean Acquisition Time) and MAC (Mean Acquisition Computation) are numerically evaluated and analyzed for widely used detection strategies in its serial and parallel search schemes. It is demonstrated that the minimized MAT and MAC are much smaller than the MAT and MAC using a detection threshold based on CFAR (Constant False Alarm Rate).**

***Index Terms*—TDCC, optimization, MAT, MAC, detection thresholds.**

## I. Introduction

Recently, following the legacy GPS, next-generation GNSS (Global Navigation Satellite System) such as modernized GPS of USA, Galileo of EU, GLONASS of Russia, Compass of China, and QZSS of Japan have been planned and being deployed [1][2]. In the next-generation GNSS, longer pseudo-random noise (PRN) code than the legacy GPS C/A (Coarse Acquisition) code are used to improve the performance of GNSS positioning. However, due to the longer PRN code, receivers in the signal acquisition process have to test a larger number of code phase hypotheses. Therefore, the signal acquisition process takes longer time or needs to have more hardware resources or computational capacity.

A number of studies for fast acquisition of GNSS signals have been introduced in the literature [3]-[7]. In general, most of the acquisition techniques can be classified into two types; the serial and parallel search schemes [8], and most of the techniques to reduce MAT (Mean Acquisition Time) and MAC (Mean Acquisition Computations) employ two sequential stages; a coarse search and a fine search. In the serial search scheme, MAT can be reduced by using two parameters; dwell time and the number of hypotheses to test. Double-dwell search technique achieves a fast acquisition by reducing the dwell time of the 1st stage [9], and to optimize the performance of the double dwell search technique, parameters such as dwell time and detection thresholds of the two stages should be properly determined. In [10], the optimization problem of determining two variables (i.e., the two thresholds) in the double dwell search technique is mathematically solved to minimize the MAT. On the other hand, TDCC (Two-Dimensional Compressed Correlator) [11]-[14] achieves a fast acquisition by compressing the number of hypotheses to test. Compared to the conventional techniques [8], TDCC has smaller MAT and MAC. However, optimal detection thresholds of TDCC should be evaluated to minimize the MAT and MAC. In the parallel search scheme, folding techniques [15][16] or TDCC can be applied to reduce the MAT and MAC, but parameters should be properly determined to optimize the performance.

Since acquisition techniques including TDCC can be implemented in various ways in terms of decision strategy, respective optimizations of acquisition performance for different decision strategies are essential. While the TC (Threshold Crossing) [9] strategy is used most in the serial search scheme, in the parallel search scheme, there are two detection strategies mostly used; MTC (Maximum Threshold Crossing) [17] and MTSMR (Maximum to Second Maximum Ratio) [18][19]. Since detection and false alarm probabilities for TC, MTC, and MTSMR are different, the performance of acquisition for TC, MTC, and MTSMR are different. Therefore, various parameters should be properly determined to minimize the MAT and MAC for TC, MTC, and MTSMR.

In this paper, optimal detection thresholds of TDCC are investigated to minimize the MAT and MAC for TC, MTC, and MTSMR. Since the performance of TDCC depends on detection thresholds, the SNR of the received signal, and the compression rate (i.e., the number of individual hypotheses in a compressed hypothesis), the optimal detection thresholds minimizing the MAT and MAC are determined with respect to the SNR of a received signal and the compression rate. The evaluation of the optimal detection thresholds minimizing the MAT and MAC is performed by numerical methods, and it is demonstrated that the minimized MAT and MAC are much smaller than the MAT and MAC using a detection threshold based on CFAR.

The rest of this paper is organized as follows. Section II introduces the concept and brief algebraic analysis of TDCC, and Section III shows the analysis of detection and false alarm

Manuscript received September 14, 2013; revised December 17, 2013; accepted December 31, 2013. The associate editor coordinating the review of this paper and approving it for publication was T. Hou.

The authors are with the CCS Graduate School for Green Transportation, Korea Advanced Institute of Science and Technology, Daejeon, Korea, 305-701 (e-mail: {vini, skong}@kaist.ac.kr). S.-H. Kong is the corresponding author.

This work (2013R1A2A2A01067863) was supported by Mid-career Researcher Program through NRF grant funded by the Korean government (MEST).

Digital Object Identifier 10.1109/TWC.2014.0204014.131704

probabilities for mostly used detection strategies. In Section IV, the optimal detection thresholds minimizing the MAT and MAC are numerically evaluated. The performance of TDCC using the optimal detection thresholds evaluated in Section IV are demonstrated with Monte Carlo simulations in Section V, and, finally, conclusion is in Section VI.

## II. Two-Dimensional Compressed Correlator

In this section, the principles of TDCC [11]-[13] are briefly introduced. TDCC exploits the fact that a hypothesis testing with a code phase and a Doppler frequency next to the true hypothesis can yield a non-negligible amount of signal energy, and the results of hypothesis testing with neighboring code phases and Doppler frequencies to the true hypothesis can be coherently combined. Therefore, a compressed hypothesis can be built to coherently combine the signal energy in a group of neighboring hypotheses, and TDCC is a correlator that tests the compressed hypothesis.

Let $r(t)$ represent a down-converted incoming signal to an IF frequency $f_{IF}$

$$r(t) = \alpha D(t-\tau)P(t-\tau)\cos(2\pi(f_{IF}+f_D)t+\theta) + n(t), \quad (1)$$

where $\alpha$, $D(t)$, $P(t)$, $\tau$, $f_D$, and $\theta$ represent the amplitude, navigation data ($R_b = \frac{1}{T_b}$ bps), PRN code ($R_c$ chip/sec (cps))($R_c = \frac{1}{T_c}$), code phase, Doppler frequency, and an unknown carrier phase of the incoming signal, respectively, and $n(t)$ is a complex additive white Gaussian noise (AWGN). Generally, to search a GNSS signal, a receiver performs a correlation between the incoming GNSS signal and a locally generated signal $r_0(t)$

$$r_0(t) = P(t-\tau_l)e^{j2\pi(f_{IF}+f_D^l)t}, \quad (2)$$

where $\tau_l$ and $f_D^l$ represents $l$-th code phase and $l$-th Doppler frequency of the locally generated signal.

In GNSS acquisition process, the Doppler frequency and code phase of the incoming signal are detected using an ACF (Auto-Correlation Function) output

$$R(\delta\tau_l, \delta f_i) \simeq \frac{\alpha D}{T}\int_{t_0}^{t_0+T} P(u)P(u-\delta\tau)e^{j(2\pi\delta f_i u+\theta)} + n(t)P(u-\tau_l)e^{-j(2\pi(f_{IF}+f_D^i)u)}du, \quad (3)$$

where $t_0$ is the time when the correlation starts, and $T$ is the correlation length, and the data $D(t)$ is regarded as a constant $D$ during the correlation length $T$ without loss of generality.

In TDCC, neighboring hypotheses are coherently compressed to reduce the MAT and MAC, so the compressed signal energy and noise variance are derived to analyze the performance. The signal energy for TDCC is [13]

$$S = \begin{cases} \sum_{i_f=0}^{m_f-1}\sum_{l_c=0}^{m_c-1} R\Big(\frac{l_c}{f_s}, \Delta f\cdot i_f\Big), & \text{minimum} \\ \sum_{i_f=0}^{m_f-1}\sum_{l_c=0}^{m_c-1} R\Big(\frac{1}{f_s}\cdot(-1)^{l_c}\cdot\Big\lfloor\frac{l_c+1}{2}\Big\rfloor, \\ \qquad \Delta f\cdot(-1)^{i_f}\cdot\Big\lfloor\frac{i_f+1}{2}\Big\rfloor\Big), & \text{maximum}, \end{cases} \quad (4)$$

where $m_c$ denotes code phase compression rate, and $m_f$ denotes Doppler frequency compression rate, $f_s$ denotes the sampling frequency, and $\Delta f$ denotes the frequency search step size. The noise variance for TDCC can be found as [13]

$$V = \sigma_f^2\sigma_c^2 f_s T N_0, \quad (5)$$

where

$$\sigma_c^2 = 2m_c - 1 \quad (6)$$

$$\sigma_f^2 = \begin{cases} 2+\frac{4}{\pi}, & \text{for } m_f = 2 \\ 3+\frac{8}{\pi}, & \text{for } m_f = 3 \\ 4+\frac{32}{3\pi}, & \text{for } m_f = 4. \end{cases} \quad (7)$$

Since the performance of TDCC depends on $m_c$, $m_f$, post-correlation SNR, and detection thresholds, the performance of TDCC should be analyzed with detection probability and false alarm probability with respect to $m_c$, $m_f$, post-correlation SNR, and detection thresholds. In the next section, detection and false alarm probabilities are derived to analyze the performance of TDCC.

## III. Detection and False Alarm Probabilities of TDCC

TDCC can be implemented in the serial and parallel search schemes. In the serial search scheme, the most widely used decision strategy is TC in which a decision variable is compared to a detection threshold. In the parallel search scheme, there are two detection strategies widely used in practice; MTC and MTSMR. In MTC, the power of the maximum ACF output is used for a decision variable and compared to a detection threshold. In MTSMR, the ratio between the power of the maximum ACF output and the power of the second maximum ACF output is compared to a detection threshold. Since MTC and MTSMR have different detection and false alarm probabilities, detection and false alarm probabilities should be derived for MTC and MTSMR.

Let $y$ denotes an ACF output from the true hypothesis, and $x$ denotes an ACF output from an incorrect hypothesis, the distribution of $Y = y^2$ is a noncentral $\chi^2$ distribution with two degrees of freedom

$$f_y(Y) = \frac{1}{V}\exp\Big(\frac{-(Y+S^2)}{V}\Big)I_0\Big(\frac{2S\sqrt{Y}}{V}\Big), \quad (8)$$

where $I_0(\cdot)$ is the zeroth-order modified Bessel function of the first kind. And the distribution of $X = x^2$ has a central $\chi^2$ distribution with two degrees of freedom

$$f_x(X) = \frac{1}{V}\exp\Big(\frac{-X}{V}\Big), \quad (9)$$

and the cumulative density function is

$$F_x(X) = 1 - \exp\Big(\frac{-X}{V}\Big). \quad (10)$$

Using $f_y$, $f_x$, and $F_x$, the false alarm, detection, and misdetection probabilities are derived in the following subsections.

### A. Serial Search

In the serial search scheme, the false alarm, detection, and misdetection probabilities are [20]

$$P_F^S(\gamma) = P\Big(X > \gamma\Big) = \exp\Big(\frac{-\gamma}{V}\Big) \tag{11a}$$

$$P_D^S(\gamma) = P\Big(Y > \gamma\Big) = Q\Big(S\sqrt{\frac{2}{V}}, \sqrt{\frac{2\gamma}{V}}\Big) \tag{11b}$$

$$P_M^S(\gamma) = 1 - P_D^S(\gamma), \tag{11c}$$

respectively, where $(\cdot)^S$ denotes the serial search scheme, and $Q(a,b)$ is the Marcum's Q-function [21] as

$$Q(a,b) = \int_b^\infty x \exp\Big(\frac{-(x^2+a^2)}{2}\Big) I_0(ax) dx. \tag{12}$$

The optimal detection threshold minimizing the MAT can obtained by numerical methods such as steepest descent algorithm which is widely used for numerical evaluation [10]. In this paper, the steepest descent algorithm is used for numerical evaluation to find a detection threshold optimizing the acquisition performance. To find the global minimum, a coarse search is applied first to find approximate detection thresholds that show the smallest MAT and MAC, where the search step size is set to 0.5 and the search is run from 0 to 10. Then, the approximate detection thresholds are used for initial points to the steepest descent algorithm used to obtain accurate optimal detection thresholds. For numerical evaluations in Section IV and Section V, derivatives of $P_F^S$ and $P_D^S$ with respect to a detection threshold $\gamma$ are obtained as

$$\frac{\partial P_F^S(\gamma)}{\partial \gamma} = -\frac{1}{V}\exp\Big(\frac{-\gamma}{V}\Big) \tag{13a}$$

$$\frac{\partial P_D^S(\gamma)}{\partial \gamma} = -\frac{1}{V}\exp\Big(\frac{-(S^2+\gamma)}{V}\Big) I_0\Big(\frac{2S\sqrt{\gamma}}{V}\Big) \tag{13b}$$

$$\frac{\partial P_M^S(\gamma)}{\partial \gamma} = -\frac{\partial P_D^S(\gamma)}{\partial \gamma}, \tag{13c}$$

respectively.

### B. Parallel Search using Maximum Threshold Crossing

In the parallel search scheme, false alarm can be occurred in two different cases; a false alarm with the incorrect Doppler frequency hypothesis with a probability $P_F$, and a false alarm with an correct Doppler frequency hypothesis with a probability $P_f$. In the parallel search scheme using the MTC detection strategy, the false alarm probability $P_F^{P1}$, detection probability $P_D^{P1}$, false alarm probability $P_f^{P1}$, and misdetection probability $P_M^{P1}$ are [17][22]

$$P_F^{P1}(\gamma) = P\Big(X^{(N/N)} > \gamma\Big) = 1 - \Big[1 - \exp\Big(\frac{-\gamma}{V}\Big)\Big]^N \tag{14a}$$

$$\begin{aligned} P_D^{P1}(\gamma) &= P\Big(Y > \gamma\Big) \cdot P\Big(Y > X^{(N-1/N-1)}\Big) \\ &= Q\Big(S\sqrt{\frac{2}{V}}, \sqrt{\frac{2\gamma}{V}}\Big) \\ &\quad \times \Big[\sum_{k=0}^{N-1}(-1)^k \binom{N-1}{k} \frac{1}{1+k} \exp\Big(\frac{-kS^2}{(1+k)V}\Big)\Big] \end{aligned} \tag{14b}$$

$$\begin{aligned} P_f^{P1}(\gamma) &= P\Big(X^{(N-1/N-1)} > \gamma\Big) \cdot P\Big(X^{(N-1/N-1)} > Y\Big) \\ &= \Big[1 - \Big(1 - \exp\Big(\frac{-\gamma}{V}\Big)\Big)^{N-1}\Big]\Bigg(1 - \Big[\sum_{k=0}^{N-1}(-1)^k \\ &\quad \times \binom{N-1}{k} \frac{1}{1+k} \exp\Big(\frac{-kS^2}{(1+k)V}\Big)\Big]\Bigg) \end{aligned} \tag{14c}$$

$$P_M^{P1}(\gamma) = 1 - P_D^{P1}(\gamma) - P_f^{P1}(\gamma), \tag{14d}$$

respectively, where $(\cdot)^{P1}$ denotes the parallel search scheme using the MTC, $N$ denotes the number of total code phase hypotheses to test, and $X^{(N/K)}$ denotes the $N$-th minimum among $K$ samples.

To obtain the optimal detection threshold minimizing the MAT using the steepest descent algorithm, derivatives of $P_F^{P1}$, $P_D^{P1}$, $P_f^{P1}$ and $P_M^{P1}$ with respect to a detection threshold $\gamma$ are obtained as

$$\frac{\partial P_F^{P1}(\gamma)}{\partial \gamma} = N\Big[1 - \exp\Big(\frac{-\gamma}{V}\Big)\Big]^{N-1} \frac{1}{V}\exp\Big(\frac{-\gamma}{V}\Big) \tag{15a}$$

$$\begin{aligned} \frac{\partial P_D^{P1}(\gamma)}{\partial \gamma} &= -\frac{1}{V}\exp\Big(\frac{-(S^2+\gamma)}{V}\Big) I_0\Big(\frac{2S\sqrt{\gamma}}{V}\Big) \\ &\quad \times \Big[\sum_{k=0}^{N-1}(-1)^k \binom{N-1}{k} \frac{1}{1+k} \exp\Big(\frac{-kS^2}{(1+k)V}\Big)\Big] \end{aligned} \tag{15b}$$

$$\begin{aligned} \frac{\partial P_f^{P1}(\gamma)}{\partial \gamma} &= N\Big[1 - \exp\Big(\frac{-\gamma}{V}\Big)\Big]^{N-1} \frac{1}{V}\exp\Big(\frac{-\gamma}{V}\Big) \\ &\quad \times \Bigg(1 - \Big[\sum_{k=0}^{N-1}(-1)^k \binom{N-1}{k} \frac{1}{1+k} \\ &\quad \times \exp\Big(\frac{-kS^2}{(1+k)V}\Big)\Big]\Bigg) \end{aligned} \tag{15c}$$

$$\frac{\partial P_M^{P1}(\gamma)}{\partial \gamma} = 1 - \frac{\partial P_D^{P1}(\gamma)}{\partial \gamma} - \frac{\partial P_f^{P1}(\gamma)}{\partial \gamma}, \tag{15d}$$

respectively.

### C. Parallel Search using Maximum to Second Maximum Ratio

In the parallel search scheme using the MTSMR detection strategy, the false alarm probability $P_F^{P2}$, detection probability $P_D^{P2}$, false alarm probability $P_f^{P2}$, and misdetection probability $P_M^{P2}$ are [19]

$$P_F^{P2}(\gamma) = P\Big(\frac{X^{(N/N)}}{X^{(N-1/N)}} > \gamma\Big) \tag{16a}$$
$$= (N^2 - N)B(N-1, 1+\gamma)$$
$$P_D^{P2}(\gamma) = P\Big(\frac{Y}{X^{(N-1/N-1)}} > \gamma\Big) \tag{16b}$$
$$= \sum_{k=0}^{N-1}(-1)^k \binom{N-1}{k} \frac{\gamma}{\gamma+k} \exp\Big(\frac{-kS^2}{V(\gamma+k)}\Big)$$
$$P_f^{P2}(\gamma) = P\Big(\frac{X^{(N-1/N-1)}}{Y} > \gamma\Big) \tag{16c}$$
$$= \int_0^\infty \int_{\gamma y}^\infty f_y(y) f_x^{(N-1)}(x) dx dy$$
$$= \int_0^\infty f_y(y) \int_{\gamma y}^\infty N-1[F_x(x)]^{N-1-1} f_x(x) dx dy$$
$$= \int_0^\infty \frac{1}{V} \exp\Big(\frac{-(y+S^2)}{V}\Big) I_0\Big(\frac{2S\sqrt{y}}{V}\Big)$$
$$\times \Big[1 - \Big(1 - \exp\Big(\frac{-y\gamma}{V}\Big)\Big)^{N-1}\Big] dy$$
$$= 1 - \sum_{k=0}^{N-1}(-1)^k \binom{N-1}{k} \frac{1}{1+\gamma k} \exp\Big(\frac{-\gamma k S^2}{(1+\gamma k)V}\Big)$$
$$P_M^{P2}(\gamma) = 1 - P_D^{P2}(\gamma) - P_f^{P2}(\gamma), \tag{16d}$$

respectively, where $(\cdot)^{P2}$ denotes the parallel search scheme using the MTSMR, and $B(\cdot,\cdot)$ is the Beta function as [23]

$$B(x,y) = \int_0^1 t^{x-1}(1-t)^{y-1} dt \tag{17}$$

for $\mathrm{Re}\{x\} > 0$ and $\mathrm{Re}\{y\} > 0$.

To obtain the optimal detection threshold minimizing the MAT using the steepest descent algorithm, derivatives of $P_F^{P2}$, $P_D^{P2}$, $P_f^{P2}$, and $P_M^{P2}$ with respect to a detection threshold $\gamma$ are obtained as

$$\frac{\partial P_F^{P2}(\gamma)}{\partial \gamma} = (N^2 - N)B(N-1, 1+\gamma)$$
$$\times(\psi(1+\gamma) - \psi(N+\gamma)) \tag{18a}$$
$$\frac{\partial P_D^{P2}(\gamma)}{\partial \gamma} = \sum_{k=0}^{N-1}(-1)^k \binom{N-1}{k} \Big[\frac{k}{(\gamma+k)^2} \exp\Big(\frac{-kS^2}{V(\gamma+k)}\Big)$$
$$+ \frac{\gamma k S^2}{V(\gamma+k)^3} \exp\Big(\frac{-kS^2}{V(\gamma+k)}\Big)\Big] \tag{18b}$$
$$\frac{\partial P_f^{P2}(\gamma)}{\partial \gamma} = -\sum_{k=0}^{N-1}(-1)^k \binom{N-1}{k} \exp\Big(\frac{-kS^2}{V(\gamma+k)}\Big)$$
$$\times\Big[\frac{-k}{(1+\gamma k)^2} - \frac{kS^2}{(1+\gamma k)^3 V}\Big] \tag{18c}$$
$$\frac{\partial P_M^{P2}(\gamma)}{\partial \gamma} = 1 - \frac{\partial P_D^{P2}(\gamma)}{\partial \gamma} - \frac{\partial P_f^{P2}(\gamma)}{\partial \gamma}, \tag{18d}$$

respectively, where $\psi(\cdot)$ is the digamma function that is defined as the logarithmic derivative of gamma function as [23]

$$\psi(x) = \frac{d}{dx}\ln\Gamma x = \frac{\Gamma'(x)}{\Gamma(x)}. \tag{19}$$

## IV. Optimization for MAT

In this section, the MAT for the serial search scheme and the MAT and MAC for the parallel search scheme are derived. To obtain the optimal detection threshold minimizing the MAT using the steepest descent algorithm, the derivatives of the MAT and MAC with respect to a detection threshold are derived.

### A. Serial Search

In the serial search scheme, when the current compressed hypothesis is correct, the 1st stage detection algorithm may or may not be able to detect the signal depending on the SNR. When the current compressed hypothesis is incorrect, the 1st stage detection algorithm may conclude the absence of signal or may generate a false alarm. When the 1st stage algorithm misses the detection, the next compressed hypothesis is tested. When the 1st stage declares a detection or generates a false alarm, the 2nd stage operation starts. Exploiting probability functions obtained in section III, the transfer functions from the beginning to the completion of acquisition can be derived [9]. The overall transfer function of TDCC is [13]

$$H^{(S)}(T) = \frac{H_D^{(S)}(T)[1 - H_0^{(S)K_1}(T)]}{K_1[1 - H_0^{(S)}(T)][1 - H_M^{(S)}(T) H_0^{(S)K_1-1}(T)]}, \tag{20}$$

where $(\cdot)^{(S)}$ denotes the serial search scheme. The correct hypothesis detection, correct hypothesis missed, and incorrect hypothesis transfer functions are derived as [13]

$$H_D^{(S)}(T) = \frac{(1 - [(1-P_F^2)T + P_F^2 T^{1+p}]^{K_2}) P_D^1 P_D^2 T^2}{K_2(1 - [(1-P_F^2)T + P_F^2 T^{1+p}])} \tag{21a}$$
$$H_M^{(S)}(T) = P_M^1 T + P_D^1 P_M^2 T^2 [(1 - P_F^2)T + P_F^2 T^{1+p}]^{K_2 - 1} \tag{21b}$$
$$H_0^{(S)}(T) = (1 - P_F^1)T + P_F^1 T[(1-P_F^2)T + P_F^2 T^{1+p}]^{K_2}, \tag{21c}$$

respectively, $K_1$ and $K_2$ denote the number of hypotheses in the 1st stage and the 2nd stage, respectively, p denotes the number of correlations for verification, and T denotes the correlation length. In this subsection, $P_F^S$ (11a) can be used for $P_F^1$, $P_F^2$, and $P_F$, $P_D^S$ (11b) can be used for $P_D^1$, $P_D^2$ and $P_D$, and $P_M^S$ (11c) can be used for $P_M^1$, $P_M^2$ and $P_M$, respectively. Then the MAT of TDCC is derived as [13]

$$\mu_T^{(S)} = \frac{dH^{(S)}(T)}{dT}\Big|_{T=1}$$
$$= \frac{1}{P_D^1 P_D^2}\Big(1 + P_D^1 + P_D^1(K_2 - 1)(1 + pP_F^2) + (K_1 - 1)$$
$$\times\big[1 + K_2 P_F^1 (1 + pP_F^2)\big]\Big) - \frac{(K_2 - 1)(1 + pP_F^2)}{2}$$
$$- \frac{(K_1 - 1)\big[1 + K_2 P_F^1 (1 + pP_F^2)\big]}{2}. \tag{22}$$

When $m_c$=1 and $m_f$=1, there is no compressed hypothesis used, the acquisition process is completed in the 1st stage, and, therefore, TDCC for $m_c = 1$ and $m_f = 1$ is equivalent to the conventional serial search scheme [8]. To derive the MAT of TDCC for $m_c$=1 and $m_f$=1, the correct hypothesis detection, correct hypothesis missed, and incorrect hypothesis transfer functions for $m_c$=1 and $m_f$=1 are derived as

$$H_D^{(S)f}(T) = P_D T^{p+1} \tag{23a}$$
$$H_M^{(S)f}(T) = P_M T \tag{23b}$$
$$H_0^{(S)f}(T) = (1 - P_F)T + P_F T^{p+1}, \tag{23c}$$

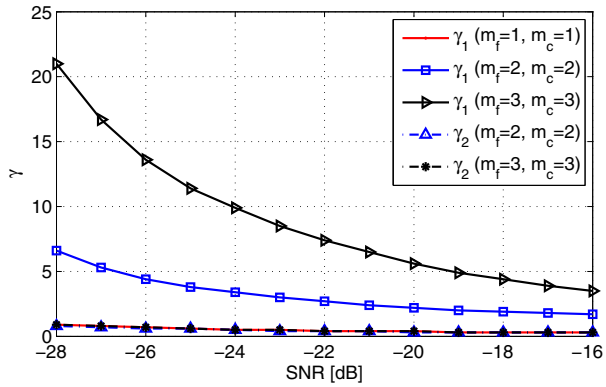


Fig. 1. Detection thresholds minimizing MAT in the serial search.

respectively, where $(\cdot)^f$ denotes the TDCC for $m_c=1$ and $m_f=1$. Then the MAT of TDCC for $m_c=1$ and $m_f=1$ is derived as [13]

$$\mu_T^{(S)f} = \left.\frac{dH^{(S)f}(T)}{dT}\right|_{T=1} = p + \frac{1}{P_D} + \left(\frac{1}{P_D} - \frac{1}{2}\right)(K_1-1)(1+pP_F). \quad (24)$$

To obtain the optimal detection thresholds minimizing the MAT using the steepest descent algorithm, derivatives of MAT with respect to the detection thresholds $\gamma_1$ and $\gamma_2$ are obtained as

$$\frac{\partial \mu_T^{(S)}}{\partial \gamma_1} = \left[\frac{(K_1-1)K_2(1+pP_F^2)(2-P_D^1P_D^2)}{2P_D^1P_D^2}\right]\frac{\partial P_F^1}{\partial \gamma_1} - \left[\frac{P_D^2(K_1-1)\left(1+K_2P_F^1(1+pP_F^2)\right)}{(P_D^1P_D^2)^2}\right]\frac{\partial P_D^1}{\partial \gamma_1} \quad (25a)$$

$$\frac{\partial \mu_T^{(S)}}{\partial \gamma_2} = \left[p(K_2-1)\left(\frac{1}{P_D^2}-\frac{1}{2}\right) + (K_1-1)pK_2P_F^1\left(\frac{2-P_D^1P_D^2}{2P_D^1P_D^2}\right)\right]\frac{\partial P_F^2}{\partial \gamma_2} - \frac{1}{P_D^1(P_D^2)^2}\Big(1+P_D^1+P_D^1(K_2-1)(1+pP_F^2) + (K_1-1)\left[1+K_2P_F^1(1+pP_F^2)\right]\Big)\frac{\partial P_D^2}{\partial \gamma_2}, \quad (25b)$$

respectively, where $\gamma_1$ and $\gamma_2$ denote the detection thresholds of the 1st stage and the 2nd stage of TDCC, respectively. In the serial search scheme, the optimal detection thresholds $\gamma_1$ and $\gamma_2$ minimizing the MAT can be numerically obtained. As shown in Fig. 1, the optimal detection thresholds $\gamma_1$ and $\gamma_2$ minimizing the MAT increase as SNR decreases, and increase as $m_cm_f$ increases. In the following figures including Fig. 1, SNR represents the pre-correlation SNR [2].

### B. Parallel Search

In the parallel search scheme, when the current compressed Doppler frequency is correct, the 1st stage detection algorithm may or may not be able to detect the signal or may generate a false alarm depending on SNR. When the 1st stage algorithm misses the detection, the next compressed Doppler frequency hypothesis is tested. When the 1st stage declares a detection or generates a false alarm, the 2nd stage operation starts.

Let $F_n$ denote the number of total Doppler frequency hypotheses, and $F_c(=F_n/m_f)$ denote the number of compressed Doppler frequency hypotheses in the 1st stage of TDCC, then the overall transfer function of TDCC is [24]

$$H^{(P)}(T) = \frac{H_D^{(P)}(T)[1-H_0^{(P)F_c}(T)]}{F_c[1-H_0^{(P)}(T)][1-H_M^{(P)}(T)H_0^{(P)F_c-1}(T)]}, \quad (26)$$

where $(\cdot)^{(P)}$ denotes the parallel search scheme. The correct hypothesis detection, correct hypothesis missed, and incorrect hypothesis transfer functions are [24]

$$H_D^{(P)}(T) \simeq P_D^1P_D^2T^{p+1} \quad (27a)$$

$$H_M^{(P)}(T) \simeq \left(P_M^1+(1-P_D^1-P_M^1)(1-P_F^2)\right)T + \left((1-P_D^1-P_M^1)P_F^2+P_D^1P_f^2\right)T^{p+1} \quad (27b)$$

$$H_0^{(P)}(T) \simeq (1-P_F^1P_F^2)T + P_F^1P_F^2T^{p+1}, \quad (27c)$$

respectively, where p denotes the number of correlations for verification, and T denotes the correlation length. In this subsection, $P_F^{P1}$ (14a) or $P_F^{P2}$ (16a) can be used to represent $P_F^1$, $P_F^2$, and $P_F$, $P_D^{P1}$ (14b) or $P_D^{P2}$ (16b) can be used to represent $P_D^1$, $P_D^2$ and $P_D$, and $P_M^{P1}$ (14d) or $P_M^{P2}$ (16d) can be used to represent $P_M^1$, $P_M^2$ and $P_M$, respectively. Then the MAT of TDCC is found as [24]

$$\mu_T^{(P)} = \left.\frac{dH^{(P)}(T)}{dT}\right|_{T=1} \simeq p+2+\frac{1}{P_D^1P_D^2}\Big[1+P_f^1+P_D^1+pP_f^1P_F^2-2P_D^1P_D^2 + (F_c-1)\Big(1-\frac{P_D^1P_D^2}{2}\Big)(1+P_F^1+pP_F^1P_F^2)\Big]. \quad (28)$$

When $m_c=1$ and $m_f=1$, there is no compressed hypothesis used, the acquisition is completed in the 1st stage. Therefore, TDCC for $m_c=1$ and $m_f=1$ is equivalent to the conventional parallel search scheme [8]. To derive the MAT of TDCC for $m_c=1$ and $m_f=1$, the correct hypothesis detection, correct hypothesis missed, and incorrect hypothesis transfer functions for $m_c=1$ and $m_f=1$ are derived as

$$H_D^{(P)f}(T) = P_DT^{p+1} \quad (29a)$$

$$H_M^{(P)f}(T) = P_MT + P_fT^{p+1} \quad (29b)$$

$$H_0^{(P)f}(T) = (1-P_F)T + P_FT^{p+1}, \quad (29c)$$

respectively. Then the MAT of TDCC for $m_c=1$ and $m_f=1$ is derived as [9]

$$\mu_T^{(P)f} = \left.\frac{dH^{(P)f}(T)}{dT}\right|_{T=1} = p+\frac{1+pP_f}{P_D}+\left(\frac{1}{P_D}-\frac{1}{2}\right)(1+pP_F)(F_n-1). \quad (30)$$

To obtain the optimal detection thresholds minimizing the MAT using the steepest descent algorithm, derivatives of the MAT with respect to detection thresholds $\gamma_1$ and $\gamma_2$ are

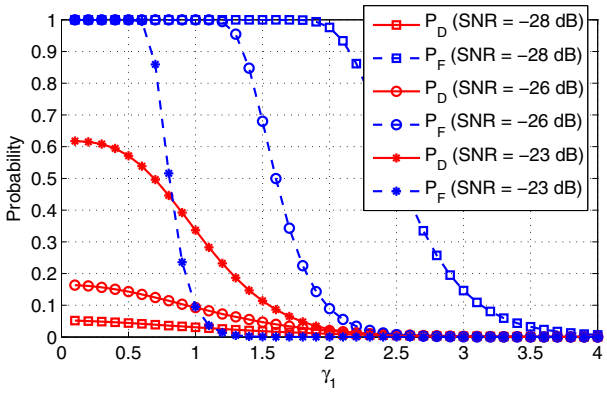


Fig. 2. $P_D$ and $P_F$ for MTC in the parallel search ($m_c = 1, m_f = 1$).

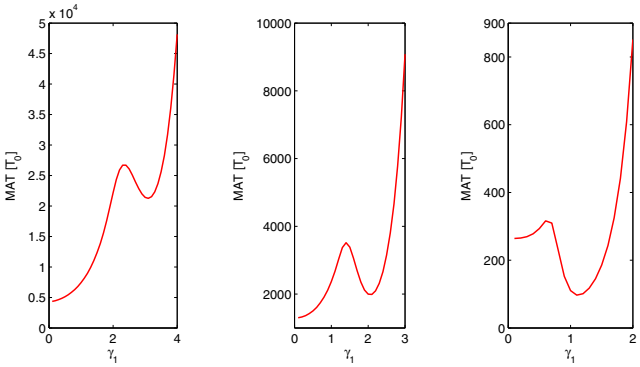


(a) SNR=−28dB (b) SNR=−26dB (c) SNR=−23dB

Fig. 3. MAT for MTC in the parallel search ($m_c = 1, m_f = 1$).

obtained as

$$\frac{\partial \mu_T^{(P)}}{\partial \gamma_1} = \left[\frac{(2-P_D^1P_D^2)(F_c-1)(1+pP_F^2)}{2P_D^1P_D^2}\right]\frac{\partial P_F^1}{\partial \gamma_1} + \frac{P_D^2}{(P_D^1P_D^2)^2}\Big[P_D^1 + (F_c-1)(1+P_F^1+pP_F^1P_F^2) - 1 - P_f^1 - pP_f^1P_F^2\Big]\frac{\partial P_D^1}{\partial \gamma_1} + \left[\frac{1+pP_F^2}{P_D^1P_D^2}\right]\frac{\partial P_f^1}{\partial \gamma_1} \quad (31a)$$

$$\frac{\partial \mu_T^{(P)}}{\partial \gamma_2} = \frac{pP_F^1}{2P_D^1P_D^2}(2F_c + P_D^1P_D^2 - F_cP_D^1P_D^2)\frac{\partial P_F^2}{\partial \gamma_2} - \frac{P_D^1}{(P_D^1P_D^2)^2}\Big[1 + P_f^1 + P_D^1 + pP_f^1P_F^2 + (F_c-1)(1+P_F^1+pP_F^1P_F^2)\Big]\frac{\partial P_D^2}{\partial \gamma_2}, \quad (31b)$$

respectively. The MAT, the detection probability $P_D$, and the false alarm probability $P_F$ for MTC with $m_c$=1 and $m_f$=1 are analyzed for the analysis of detection thresholds $\gamma_1$ and $\gamma_2$ to minimize the MAT. In general, MAT depends on $P_F$ and $P_D$; MAT decreases as $P_F$ decreases or $P_D$ increases. $P_D$ and $P_F$ decrease as the detection thresholds $\gamma_1$ and $\gamma_2$ increase, however, $P_F$ decreases faster than $P_D$. When SNR is $-26$dB as shown in Fig. 2, $P_F$ is about 1 and $P_D$ gradually decreases for $\gamma_1 < 1.3$ so that the MAT increases as $\gamma_1$ increases as shown in Fig. 3(b). For $1.3 < \gamma_1 < 2$, $P_F$ starts to decreases rapidly so that the MAT decreases from about 3800 to 2000 as $\gamma_1$ increases as shown in Fig. 2 and Fig. 3(b). For $\gamma_1 > 2$, $P_F$ starts to saturate at 0 and $P_D$ is decreasing slowly so that the MAT increases again as $\gamma_1$ increases as shown in Fig. 2 and Fig. 3(b). Depending on the different behaviors of the $P_D$ and $P_F$ at different SNR, the minimum MAT can be located at $\gamma_1 = 0$ or $\gamma_1 > 0$. For example, the optimal detection threshold $\gamma_1$ minimizing the MAT with $m_c$=1 and $m_f$=1 is 0 for low SNR ($< -25$dB) and larger than 0 for high SNR ($> -25$dB) as shown in Fig. 3(a) and Fig. 3(c), respectively. This tendency can be found in the graph of optimal detection threshold $\gamma_1$ minimizing the MAT as well.

In Fig. 4(a), numerically evaluated optimal detection thresholds $\gamma_1$ and $\gamma_2$ minimizing the MAT for MTC are shown, and as analyzed above, the optimal detection threshold $\gamma_1$ minimizing the MAT is 0 for low SNR ($< -25$dB) and larger than 0 for high SNR ($> -25$dB) when $m_c$=1 and $m_f$=1. For all combinations of $m_c$ and $m_f$, when SNR is not low, the optimal detection threshold $\gamma_1$ minimizing the MAT increases as SNR decreases. And the optimal detection threshold $\gamma_1$ minimizing the MAT increases as $m_cm_f$ increases. However, the optimal detection threshold $\gamma_1$ minimizing the MAT is zero for low SNR. Denoting $S_\gamma$ the SNR at which $\gamma_1$ jumps up to a positive value from zero, it can be found that $S_\gamma$ increases as $m_cm_f$ increases. On the other hand, the optimal detection threshold $\gamma_2$ increases as SNR decreases in all SNR range, and the optimal detection threshold $\gamma_2$ is almost the same for different combinations of $m_c$ and $m_f$ as long as $m_cm_f \ll N$.

The optimal detection thresholds $\gamma_1$ and $\gamma_2$ minimizing the MAT for MTSMR are shown in Fig. 4(b). The legend in Fig. 4(b) is the same as that in Fig. 4(a). The 2nd stage uses MTC, since a small number of individual hypotheses are tested ($m_cm_f \ll N$). As shown, the optimal detection threshold $\gamma_1$ minimizing the MAT decreases, and is saturated at about 1.2 as SNR decreases, and the optimal detection threshold $\gamma_2$ is almost the same for different combinations of $m_c$ and $m_f$ as long as $m_cm_f \ll N$.

## V. Optimization for MAC

In the parallel search scheme, the MAC as well as the MAT are important criteria to evaluate the performance of acquisition, and, therefore, the optimal values of $\gamma_1$ and $\gamma_2$ that minimize the MAC are numerically evaluated in this section. Let $N_f$, $N_s$ and $N_p$ denote the computational complexities in the first, second, and verification stages, respectively.

The overall transfer function related to the computational complexity of TDCC in the parallel search scheme can be found as [14]

$$G^{(P)}(C) = \frac{G_D^{(P)}(C)[1-G_0^{(P)F_c}(C)]}{F_c[1-G_0^{(P)}(C)][1-G_M^{(P)}(C)G_0^{(P)(F_c-1)}(C)]}. \quad (32)$$

The correct hypothesis detection, correct hypothesis missed,

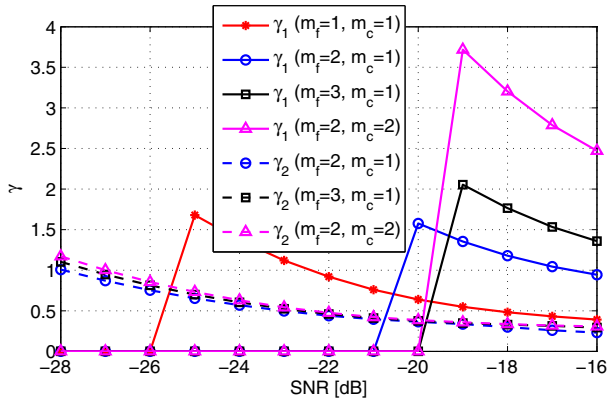


(a) Detection thresholds for MTC

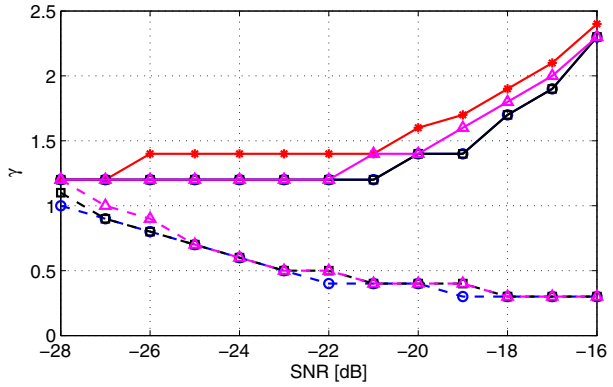


(b) Detection thresholds for MTSMR

Fig. 4. Detection thresholds minimizing MAT in the parallel search.

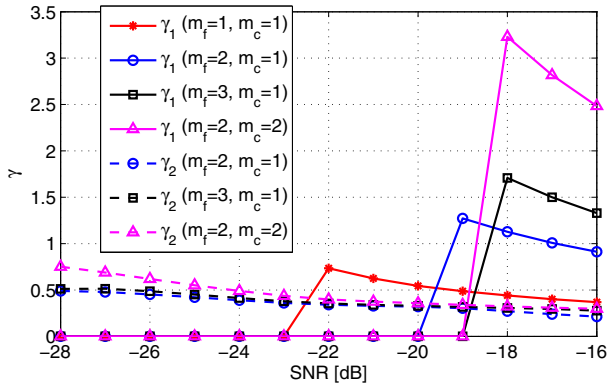


(a) Detection thresholds for MTC

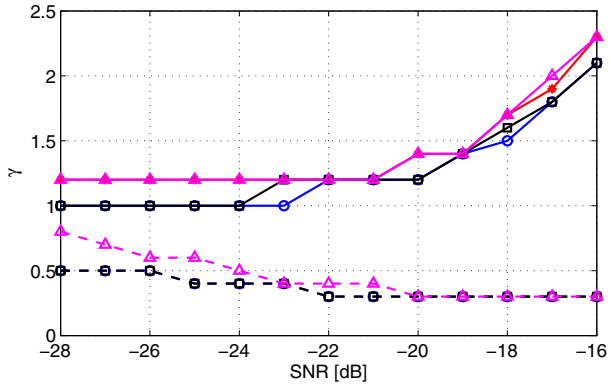


(b) Detection thresholds for MTSMR

Fig. 5. Detection thresholds minimizing MAC in the parallel search.

and incorrect hypothesis transfer functions are derived as [14]

$$G_D^{(P)}(C) = P_D^1 P_D^2 P_D^V C^{N_f} C^{N_s} C^{N_p} \simeq P_D^1 P_D^2 C^{N_f} C^{N_s} C^{N_p} \quad (33a)$$

$$G_M^{(P)}(C) = P_M^1 C^{N_f} + (1-P_D^1-P_M^1)(1-P_F^2)C^{N_f} C^{N_s} + [(1-P_D^1-P_M^1)P_F^2 + P_D^1 P_f^2] \times (1-P_f^v) C^{N_f} C^{N_s} C^{N_p} \quad (33b)$$

$$G_0^{(P)}(C) = (1-P_F^1 P_F^2) C^{N_f} C^{N_s} + (P_F^1 P_F^2)(1-P_F^v) C^{N_f} C^{N_s} C^{N_p}, \quad (33c)$$

respectively, and $C$ denote the unit computational complexity for one complex multiplication. In this subsection, $P_F^{P1}$ (14a) or $P_F^{P2}$ (16a) can be used for $P_F^1$, $P_F^2$, and $P_F$, $P_D^{P1}$ (14b) or $P_D^{P2}$ (16b) can be used for $P_D^1$, $P_D^2$ and $P_D$, and $P_M^{P1}$ (14d) or $P_M^{P2}$ (16d) can be used for $P_M^1$, $P_M^2$ and $P_M$, respectively. And the MAC is derived as [14]

$$\mu_C^{(P)} = \left.\frac{dG^{(P)}(C)}{dC}\right|_{C=1} = N_p - \frac{F_c-1}{2}(N_f + N_s P_F^1 + N_p P_F^1 P_F^2) + \frac{1}{P_D^1 P_D^2}\big[F_c N_f + (P_D^1 + P_f^1) N_s + P_f^1 P_F^2 N_p + (F_c-1)(N_s P_F^1 + N_p P_F^1 P_F^2)\big]. \quad (34)$$

When $m_c$=1 and $m_f$=1, there is no compressed hypothesis used, the acquisition is completed in the 1st stage. Therefore, TDCC for $m_c$=1 and $m_f$=1 is equivalent to the conventional parallel search scheme [8]. To derive the MAC of TDCC for $m_c$=1 and $m_f$=1, the correct hypothesis detection, correct hypothesis missed, and incorrect hypothesis transfer functions for $m_c$=1 and $m_f$=1 are derived as

$$G_D^{(P)f}(C) = P_D C^{N_f+N_p} \quad (35a)$$

$$G_M^{(P)f}(C) = P_M C^{N_f} + P_f C^{N_f+N_p} \quad (35b)$$

$$G_0^{(P)f}(C) = (1-P_F) C^{N_f} + P_F C^{N_f+N_p}, \quad (35c)$$

respectively, where $(\cdot)^f$ denotes the TDCC for $m_c=1$ and $m_f=1$. Then the MAC of TDCC for $m_c=1$ and $m_f=1$ is derived as [14]

$$\mu_C^{(P)f} = \left.\frac{dG^{(P)f}(C)}{dT}\right|_{C=1} = N_p\big(1+\frac{P_f}{P_D}\big) + N_f\big(\frac{1}{P_D}\big) + (F_n-1) \times (N_f + N_p P_F)\big(\frac{1}{P_D} - \frac{1}{2}\big). \quad (36)$$

To obtain the optimal detection thresholds minimizing the MAC using the steepest descent algorithm, derivatives of the MAC with respect to detection thresholds $\gamma_1$ and $\gamma_2$ are

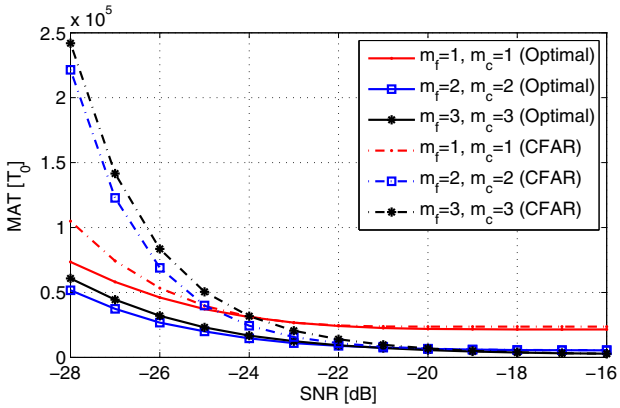


Fig. 6. MAT in the serial search.

obtained as

$$\frac{\partial \mu_C^{(P)}}{\partial \gamma_1} = \left[\frac{(F_c-1)(2-P_D^1P_D^2)(N_s+N_pP_F^2)}{2P_D^1P_D^2}\right]\frac{\partial P_F^1}{\partial \gamma_1} + \left[\frac{N_s}{P_D^1P_D^2}\right]\frac{\partial P_f^1}{\partial \gamma_1} - \frac{P_D^2}{(P_D^1P_D^2)^2}\Big[F_cN_f + P_f^1N_s + P_f^1P_F^2N_p + (F_c-1)(N_sP_F^1 + N_pP_F^1P_F^2)\Big]\frac{\partial P_D^1}{\partial \gamma_1} \quad (37a)$$

$$\frac{\partial \mu_C^{(P)}}{\partial \gamma_2} = \left[\frac{N_pP_F^1(F_c-1)(2-P_D^1P_D^2)+2N_pP_f^1}{2P_D^1P_D^2}\right]\frac{\partial P_F^2}{\partial \gamma_2} + \frac{P_D^1}{(P_D^1P_D^2)^2}\Big[F_cN_f + (P_D^1+P_f^1)N_s + P_f^1P_F^2N_p + (F_c-1)(N_sP_F^1 + N_pP_F^1P_F^2)\Big]\frac{\partial P_D^2}{\partial \gamma_2}, \quad (37b)$$

respectively. In the parallel search scheme, the optimal detection thresholds $\gamma_1$ and $\gamma_2$ minimizing the MAC can be numerically obtained as shown in Fig. 5, which shows a similar pattern of the detection thresholds $\gamma_1$ and $\gamma_2$ minimizing the MAT with respect to SNR.

## VI. Numerical Results

In this section, TDCC is tested for a receiver with 4MHz BPF bandwidth, sampling frequency $f_s = 2R_c$, correlation length $T = T_0$(1msec), and code phase and Doppler frequency search step sizes $0.5T_c$ and $\Delta f = 500$Hz, respectively, trying to acquire an incoming PRN code signal that has a chip rate $R_c = 1$MHz and an unknown Doppler frequency within $[-5, 5]$kHz. The performance of detection thresholds $\gamma_1$ and $\gamma_2$ minimizing the MAT and MAC evaluated in Section IV and V are demonstrated with Monte Carlo simulations.

As shown in Fig. 6, the minimized MAT in the serial search scheme is generally smaller than that using a detection threshold based on CFAR (Constant False Alarm Rate) ($P_F = 0.01$). The minimized MAT is similar to and much smaller than the MAT using a detection threshold based on CFAR for high SNR ($> -20$dB) and low SNR ($< -20$dB), respectively. In addition, the MAT increases as $m_cm_f$ increases when a detection threshold based on CFAR is used for low SNR. On the contrary, the minimized MAT of TDCC for $m_cm_f > 1$ is smaller than that of the TDCC for $m_cm_f = 1$.

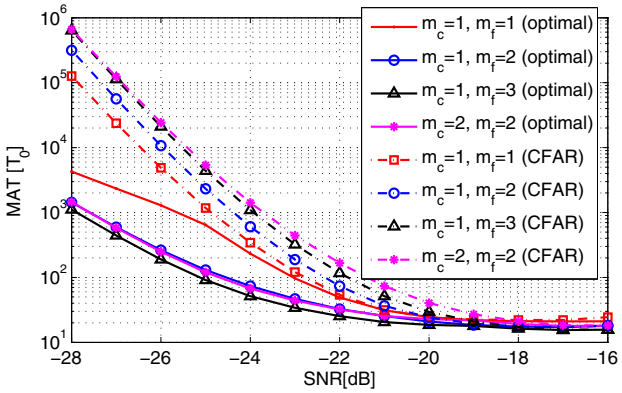


(a) MAT for MTC

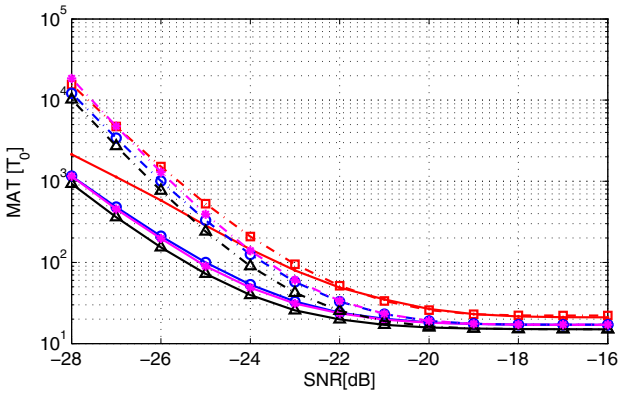


(b) MAT for MTSMR

Fig. 7. MAT in the parallel search.

As shown in Fig. 7, the minimized MAT in the parallel search scheme is smaller than that using a threshold based on CFAR (Constant False Alarm Rate) ($P_F = 0.01$). Fig. 7(a) and Fig. 7(b) show the performance of the minimized MAT for MTC and MTSMR, respectively. The legend in Fig. 7(b) is the same as that in Fig. 7(a). The minimized MAT is similar to and much smaller than the MAT using a detection threshold based on CFAR for high SNR ($> -20$dB) and low SNR ($< -20$dB), respectively, for both MTC and MTSMR. In the case of MAT for MTC, when a detection threshold based on CFAR is used, the MAT increases as $m_cm_f$ increases for low SNR, however, the minimized MAT of TDCC for $m_cm_f > 1$ is generally smaller than that of TDCC for $m_cm_f = 1$.

The minimized MAC in the parallel search scheme is smaller than that using a detection threshold based on CFAR (Constant False Alarm Rate) ($P_F = 0.01$) as shown in Fig. 8. Fig. 8(a) shows the performance of the minimized MAC for MTC, and Fig. 8(b) shows the performance of the minimized MAC for MTSMR. The legend in Fig. 8(b) is the same as that in Fig. 8(a). Similar to the observation with the minimized MAT in Fig. 7, the minimized MAC is similar to and much smaller than the MAC using a detection threshold based on CFAR for high SNR ($> -20$dB) and low SNR ($< -20$dB), respectively, for both MTC and MTSMR. In the case of the MAC for MTC, when a detection threshold based on CFAR is used, the MAC increases as $m_cm_f$ increases for low SNR, however, the minimized MAC of TDCC for $m_cm_f > 1$ is

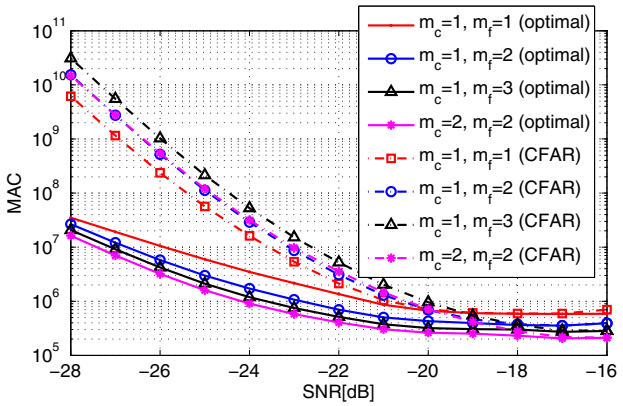


(a) MAC for MTC

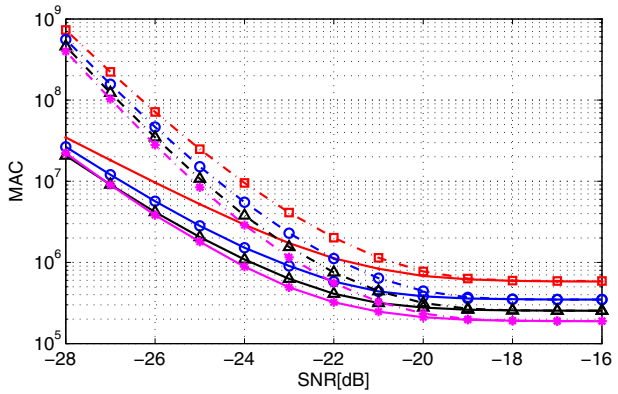


(b) MAC for MTSMR

Fig. 8. MAC in the parallel search.

smaller than that of TDCC for $m_c m_f = 1$.

The optimal detection thresholds $\gamma_1$ and $\gamma_2$ to minimize the MAT and MAC can be numerically modeled to $\gamma_M$ as

$$\gamma_M = C_c \exp\left(-C_a \text{SNR}/10 + C_b\right) + C_d, \tag{38}$$

where $C_a, C_b, C_c$, and $C_d$ are unknown coefficients, and SNR represents the pre-correlation SNR. The coefficients of $\gamma_M$ can be numerically determined to have minimum mean square error with the optimal detection thresholds $\gamma_1$ and $\gamma_2$ that are numerically evaluated in Section IV and V. Table I provides the coefficients of the equation (38) and $S_\gamma$ for $\gamma_1$. Note that, in the case of the parallel search scheme using MTC shown in Fig. 4(a) and Fig. 5(a), $\gamma_M$ is found only for the non-zero values of the detection thresholds $\gamma_1$ and $\gamma_2$ minimizing the MAT or MAC (i.e., SNR $> S_\gamma$). As we denote $S_\gamma$ the SNR where $\gamma_1$ changes from $\gamma_1 > 0$ to (or from) $\gamma_1 = 0$ suddenly, $\gamma_M$ can be used for $\gamma_1$ when SNR$> S_\gamma$. In table I, $S_\gamma$ of MAT is denoted as $S_\gamma^T$, and $S_\gamma$ of MAC is represented by $S_\gamma^C$.

## VII. Conclusion

The optimal detection thresholds minimizing the MAT and MAC for TDCC are obtained and analyzed via numerical evaluation for widely used detection strategies, such as TC, MTC, and MTSMR, in the serial and parallel search schemes. Since the performance of TDCC depends on detection thresholds, SNR, and compression rate, the optimal detection thresholds minimizing the MAT and MAC should be properly determined with respect to the SNR and the compression rate.

TABLE I
Table for Coefficients in (38)

| | $[m_c, m_f, S_\gamma^T, S_\gamma^C]$ | $C_a$ | $C_b$ | $C_c$ | $C_d$ |
|---|---|---|---|---|---|
| $[\gamma_1,\gamma_2]$ for MAT in Serial Search | [1,1,,] | [1.5,] | [2.9,] | [0.1,] | [0.4,] |
| | [1,2,,] | [1.9,1.1] | [2.8,3.0] | [0.1,0.2] | [0.5,0.4] |
| | [1,3,,] | [2.1,1.4] | [2.8,2.8] | [0.1,0.1] | [0.7,0.4] |
| | [2,1,,] | [1.9,1.1] | [2.8,2.3] | [0.1,0.1] | [0.5,0.4] |
| | [2,2,,] | [2.4,1.5] | [2.8,3.0] | [0.1,0.1] | [1.4,0.4] |
| | [2,3,,] | [1.1,1.5] | [2.2,2.9] | [2.5,0.1] | [-0.1,0.4] |
| | [3,1,,] | [2.2,1.4] | [3.0,2.8] | [0.1,0.1] | [0.7,0.4] |
| | [3,2,,] | [0.6,1.5] | [0.6,2.9] | [2.6,0.1] | [-2.2,0.4] |
| | [3,3,,] | [2.2,1.5] | [2.9,2.9] | [0.7,0.1] | [2.3,0.4] |
| $\gamma_1$ for [MAT,MAC] in Parallel Search (MTC) | [1,1,-25,-22] | [2.0,1.8] | [2.5,2.4] | [0.1,0.1] | [0.1,0.2] |
| | [1,2,-20,-19] | [1.5,0.3] | [2.3,-1.6] | [0.8,0.4] | [0,-2.3] |
| | [1,3,-19,-18] | [2.5,2.6] | [2.8,2.6] | [0.2,0.1] | [0.7,0.8] |
| | [2,1,-20,-19] | [2.3,2.5] | [3.0,3.0] | [0.2,0.1] | [0.5,0.6] |
| | [2,2,-19,-18] | [2.5,0.6] | [3.0,0.2] | [0.4,2.2] | [0.4,-2.3] |
| | [2,3,-19,-18] | [-3.0,-3.0] | [-3.0,-3.0] | [0,0] | [0.1,0.1] |
| $\gamma_2$ for [MAT,MAC] in Parallel Search (MTC) | [1,2,,] | [1.3,0.4] | [2.7,0.4] | [0.4,0.4] | [0,-0.3] |
| | [1,3,,] | [1.8,0.8] | [2.9,2.7] | [0.1,0.7] | [0.2,0.1] |
| | [2,1,,] | [1.3,1] | [2.7,2.8] | [0.4,0.7] | [0,0] |
| | [2,2,,] | [1.7,1.7] | [2.4,3.0] | [0.1,0.1] | [0.1,0.2] |
| | [2,3,,] | [1.7,1.2] | [2.3,2.8] | [0.1,0.4] | [0.1,0.1] |
| $\gamma_1$ for [MAT,MAC] in Parallel Search (MTSMR) | [1,1,,] | [-2.7,-4.8] | [-2.8,-6] | [5.4,6] | [1.2,1.2] |
| | [1,2,,] | [-4.8,-3.8] | [-6,-5.5] | [6,2] | [1.2,1] |
| | [1,3,,] | [-4.8,-3.4] | [-6,-5.9] | [6,0.7] | [1.2,1] |
| | [2,1,,] | [-3.1,-3.5] | [-3.4,-4.2] | [5.8,5.2] | [1.1,1] |
| | [2,2,,] | [-3.1,-4.7] | [-3.4,-6] | [5.8,5.2] | [1.1,1.2] |
| | [2,3,,] | [-3.1,-4.6] | [-3.4,-6] | [5.8,4.5] | [1.1,1.2] |

In the serial search scheme using TC, the optimal detection thresholds minimizing the MAT decrease as SNR increases, and increase as the compression rate increases. In the parallel search scheme using MTC, the optimal detection thresholds minimizing the MAT and MAC increase as SNR decreases and as the compression rate increases but are zero for low SNR. In the parallel search scheme using MTSMR, the optimal detection thresholds minimizing the MAT and MAC decrease as SNR decreases, and are similar for different choice of $m_c$ and $m_f$. It is demonstrated that the minimized MAT and MAC are smaller than the MAT and MAC using a detection threshold based on CFAR.

## References

[1] E. D. Kaplan and C. J. Hegarty, *Understanding GPS: Principles and Applications*, 2nd ed. Artech House, 2005.
[2] F. V. Diggelen, *A-GPS: Assisted GPS, GNSS, and SBAS*. Artech House, 2009.
[3] J. Yi, *et al.*, "A new FFT-based acquisition algorithm for GPS signals," in *2008 Education Technol. Training, 2008. and 2008 International Workshop Geoscience Remote Sensing. ETT and GRS 2008* International Workshop on. vol. 2. IEEE, 2008.
[4] D. Akopian, "Fast FFT based GPS satellite acquisition methods," *IEE Proc.-Radar Sonar Navig.*, vol. 152, no. 4, Aug. 2005.
[5] Y. Huang and J. Wang, "Rapid search methods for code acquisition in UWB impulse radio communications," *IEEE Trans. Wireless Commun.*, vol. 6, no. 10, pp. 3578–3588, Oct. 2007.
[6] S. Yeom, Y. Jung, and S. Lee, "An adaptive threshold technique for fast PN code acquisition in DS-SS systems," *IEEE Trans. Veh. Technol.*, vol. 60, no. 6, pp. 2870–2875, July 2011.
[7] K. M. Chugg and M. Zhu, "A new approach to rapid PN code acquisition using iterative message passing techniques," *IEEE J. Sel. Areas Commun.*, vol. 23, no. 5, pp. 884–897, May 2005.
[8] K. Borre, D. Akos, N. Bertelsen, P. Rinder, and S. Jensen, *A Software Defined GPS and Galileo Receiver: A Single Frequency Approach*. Birkhauser, 2007.
[9] A. J. Viterbi, *CDMA: Principles of Spread Spectrum Communication*. Addison-Wesley Publishing Company, 1995.

[10] G. Giunta, A. Neri, and M. Carli, "Constrained optimization of non-coherent serial acquisition of spread-spectrum code by exploiting the generalized Q-functions," *IEEE Trans. Veh. Technol.*, vol. 52, no. 5, pp. 1378–1385, Sept. 2003.
[11] B. Kim and S.-H. Kong, "Two dimensional compressed correlator for fast acquisition in GNSS," in *Proc. 2013 ION ITM.*
[12] B. Kim and S.-H. Kong, "FFT based two dimensional compressed correlator for fast acquisition in GNSS," in *Proc. 2013 ION PNT.* 2013.
[13] S.-H. Kong and B. Kim, "Two dimensional compressed correlator for fast acquisition in GNSS," *IEEE Trans. Wireless Commun.*, vol. 12, no. 11, pp. 5859–5867, Nov. 2013.
[14] B. Kim and S.-H. Kong, "Low computational BOC(m,n) signal acquisition in the presence of tiered code," *IEEE Trans. Wireless Commun.*, submitted.
[15] C. Yang, J. Vasquez, and J. Chaffee, "Fast direct P(Y)-code acquisition using XFAST," in *Proc. 1999 ION GPS*, pp. 317–324.
[16] H. Li, X. Cui, M. Lu, and Z. Feng, "Dual-folding based rapid search method for long PN-code acquisition," *IEEE Trans. Wireless Commun.*, vol. 7, no. 12, pp. 5286–5296, Dec. 2008.
[17] G. E. Corazza, "On the MAX/TC criterion for code acquisition and its application to DS-SSMA systems," *IEEE Trans. Wireless Commun.*, vol. 44, no. 9, pp. 1173–1182, Sept. 1996.
[18] B. Geiger, M. Soudan, and C. Vogel, "On the detection probability of parallel code phase search algorithms in GPS receivers," in *2010 IEEE International Symp. Personal, Indoor, Mobile Radio Commun.*
[19] B. Geiger, C. Vogel, and M. Soudan, "Comparison between ratio detection and threshold comparison for GNSS acquisition," *IEEE Trans. Aero. Electron. Syst.*, vol. 48, no. 2, pp. 1772–1779. Apr. 2012.
[20] M. A. Abu-Rgheff, *Introduction to CDMA Wireless Communications*. Academic Press, 2007.
[21] J. I. Marcum, *A Table of Q-functions*, Rand Corp. Report, RM-339, Jan. 1950.
[22] H. A. David and H. N. Nagaraja, *Order Statistics*, 3rd ed. John Wiley and Sons, 2003.
[23] A. Papoulis, *Probability, Random Variables, and Stochastic Process*, 2nd ed. Prentice Hall, 1992.
[24] E. A. Sourour and S. C. Gupta, "Direct-sequence spread-spectrum parallel acquisition in a fading mobile channel," *IEEE Trans. Commun.*, vol. 38, no. 7, pp. 992–998, July 1990.

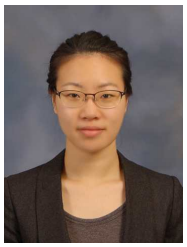

**Binhee Kim** (S'08) received a B.S.E.E.and M.S.E.E. from the Korea Advanced Institute of Science and Technology (KAIST), Korea, in 2008 and 2010, respectively. She is currently pursuing the Ph.D. degree at The CCS Graduate School for Green Transportation in the KAIST. Her research interests include super-resolution signal processing, detection and estimation in next-generation GNSS.

**Seung-Hyun Kong** (M'06) received a B.S.E.E. from the Sogang University, Korea, in 1992, an M.S.E.E. from the Polytechnic University, New York, in 1994, and a Ph.D. degree in Aeronautics and Astronautics from Stanford University, CA, in 2006. From 1997 to 2004, he was with Samsung Electronics Inc. and Nexpilot Inc., both in Korea, where his research focus was on wireless communication systems and mobile positioning technologies. In 2006, he was involved with hybrid positioning technology development using wireless location signature and Assisted GNSS at Polaris Wireless, Inc., Santa Clara, and from 2007 to 2009, he was a research staff at Corporate R&D of Qualcomm Inc., San Diego, where his R&D focus was on the indoor location technologies and advanced GNSS technologies. Since 2010, he has been an Assistant Professor at The CCS Graduate School for Green Transportation in the Korea Advanced Institute of Science and Technology (KAIST). His research interests include super-resolution signal processing, detection and estimation in navigation systems, and vehicular communication systems.